Bol. Soc. Mat. Mex. (2024) 30:38
https://doi.org/10.1007/s40590-024-00617-4

Sociedad Matemática Mexicana

ORIGINAL ARTICLE

Geodesic complexity of a cube

Donald M. Davis[1]

Received: 17 August 2023 / Accepted: 14 March 2024 / Published online: 10 April 2024

Abstract
The topological (resp. geodesic) complexity of a topological (resp. metric) space is roughly the smallest number of continuous rules required to choose paths (resp. shortest paths) between any points of the space. We prove that the geodesic complexity of a 3-dimensional cube exceeds its topological complexity by exactly 2. The proof involves a careful analysis of cut loci of the cube.

Keywords Geodesic complexity · Topological robotics · Geodesics · Cut locus · Cube

Mathematics Subject Classification 53C22 · 52B10 · 55M30

1 Introduction

In [6], Farber introduced the concept of the *topological complexity*, $\mathrm{TC}(X)$, of a topological space X, which is the minimal number k, such that there is a partition

$$X \times X = E_1 \sqcup \cdots \sqcup E_k$$

with each E_i being locally compact and admitting a continuous function $\phi_i : E_i \to P(X)$, such that $\phi_i(x_0, x_1)$ is a path from x_0 to x_1. Here, $P(X)$ is the space of paths in X with the compact-open topology, and each ϕ_i is called a motion-planning rule. If X is the space of configurations of one or more robots, this models the number of continuous rules required to program the robots to move between any two configurations.

Recio-Mitter [8] suggested that if X is a metric space, then we require that the paths $\phi_i(x_0, x_1)$ be minimal geodesics (shortest paths) from x_0 to x_1, and defined the *geodesic complexity*, $\mathrm{GC}(X)$, to be the smallest number k, such that there is a partition

$$X \times X = E_1 \sqcup \cdots \sqcup E_k$$

✉ Donald M. Davis
dmd1@lehigh.edu

[1] Department of Mathematics, Lehigh University, Bethlehem, PA 18015, USA

with each E_i being locally compact and admitting a continuous function $\phi_i : E_i \to P(X)$, such that $\phi_i(x_0, x_1)$ is a minimal geodesic from x_0 to x_1.[1] Each function ϕ_i is called a *geodesic motion-planning rule* (GMPR).

One example discussed by Recio-Mitter [8] was when X is (the surface of) a cube. It is well known that here $\mathrm{TC}(X) = \mathrm{TC}(S^2) = 3$, and he showed that $\mathrm{GC}(X) \geq 4$. In this paper, we prove that in this case, $\mathrm{GC}(X) = 5$.

Theorem 1.1 *If X is a cube, then* $\mathrm{GC}(X) = 5$.

For comparison, in [3], the author proved that for a regular tetrahedron T, $\mathrm{GC}(T) = 4$ or 5, but was not able to establish the precise value. Here again, $\mathrm{TC}(T) = \mathrm{TC}(S^2) = 3$.

Our work relies heavily on the work of the author and Guo [4], where they analyzed the isomorphism classes of cut loci on the cube as labeled graphs. In Sect. 2, we review the relevant parts of that work. In Sect. 3, we prove that $\mathrm{GC}(X) \leq 5$ by constructing five explicit geodesic motion-planning rules. In Sect. 4, we prove $\mathrm{GC}(X) \geq 5$, using methods similar to those used in [3, 8].

2 Background on cut loci of a cube

In this section, we present background material, mostly from [4], regarding cut loci for a cube. The distance, $d(P, Q)$, between points on the cube is the Euclidean distance for points on the same face, while for any points, it is $\min(\sum_{i=0}^{n-1} d(P_i, P_{i+1}))$, over all sequences with $P_0 = P$, $P_n = Q$, and P_i and P_{i+1} in the same face.

The *cut locus* of a point P on a polyhedron, denoted L_P, is the closure of the set of points Q, such that there is more than one shortest path (minimal geodesic) from P to Q. The cut locus is a labeled graph with corner points of the polyhedron labeling the leaves ([9, Corollary of Lemma 4.4]). It is possible that a degree-2 vertex of the graph might also be labeled by a corner point. Two labeled graphs are isomorphic if there is a graph bijection between them preserving labels. We let $\mathbf{L}$ denote the isomorphism class of a cut locus.

Figure 1, from [4], shows the partition of a face of a cube into 193 connected subsets with constant $\mathbf{L}$. Figure 2, also from [4], is a reparametrized version of the regions in the left quadrant of Fig. 1.

In [4], we listed, in stylized form, the $\mathbf{L}$ for the various regions, but here, as we are interested in continuity of motion-planning rules, we are concerned about other aspects, such as the placement of edges of the cut locus with respect to one another.

The cut loci are found by the method of star unfolding and Voronoi diagrams, as developed in [1, 7]. We will use the same numbering of the corner points of the cube as was used in [4] and appears in Fig. 3, also taken from [4], which, for future reference, includes an example of the cut locus of the midpoint of edge 5–8.

In [4], we explain how the diagram on the right side of Fig. 4 is obtained, depicting in bold red the cut locus of the point P in the left side of Fig. 4. The numbers at half

[1] Recio-Mitter's definition of $\mathrm{GC}(X) = k$ involved partitions into sets $E_0, \ldots, E_k$, which, for technical reasons, has become the more common definition of concepts of this sort, but we prefer here to stick with Farber's more intuitive formulation.

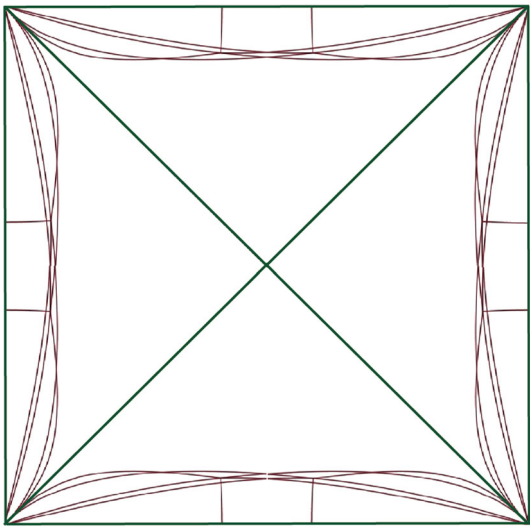

Fig. 1 Decomposition of a face into subsets on which **L** is constant

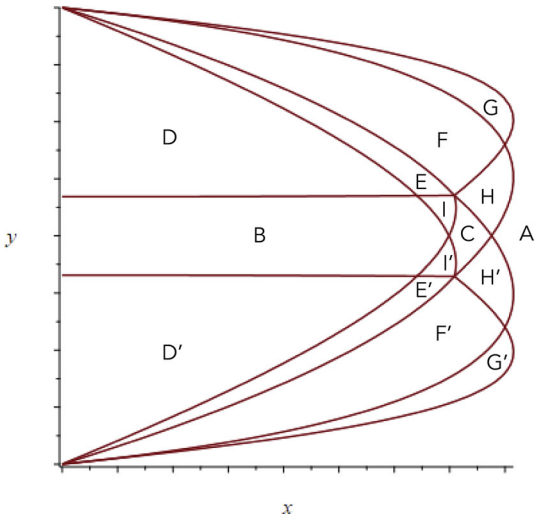

Fig. 2 Regions in left quadrant of Fig. 1

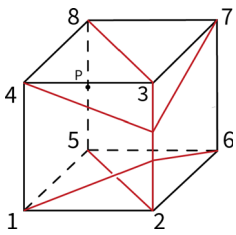

Fig. 3 A cube with labeled corner points, and the cut locus for the middle point of an edge highlighted

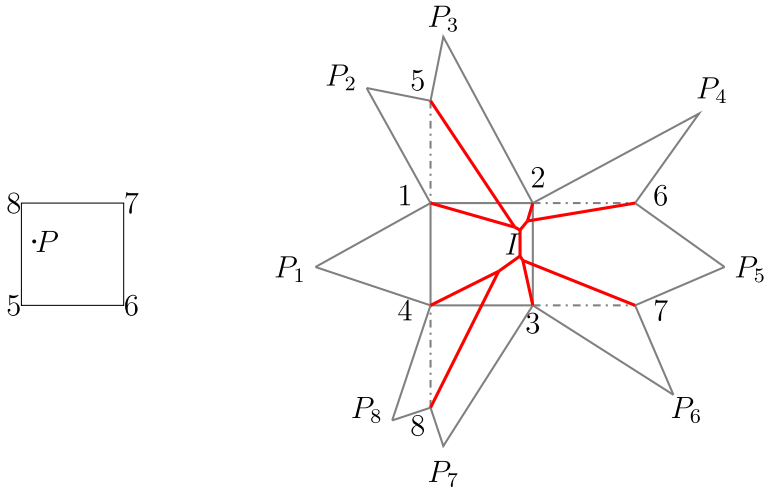

Fig. 4 Voronoi cells and cut locus of P

of the vertices of the polygon correspond to the corner points in Fig. 3, and the labels $P_1, \ldots, P_8$ at the other vertices are different positions of the point P in an unfolding of the cube. Every point of the cube occurs exactly once inside or on the 16-gon in Fig. 4, except that some occur on two boundary segments, and P occurs eight times. Note that the boundary segments of the polygon in Fig. 4 are straight line segments from P to corner points of the cube.

For example, the region in the right side of the 16-gon in Fig. 4 bounded above and below by the segments coming in from the vertices labeled 6 and 7, on the right by P_5, and on the left by the short vertical segment I is all the points that are closer to the P_5 version of point P than to the others. This is called the Voronoi cell of P_5. The segment I is equally close to versions P_1 and P_5. There are two equal minimal geodesics from P to points on I; one crosses the segment connecting corner points 1 and 4, while the other crosses the segment connecting 6 and 7.

It is proved in [5] that the top and bottom halves of cut loci of the cube can be considered separately. Although all the regions in Fig. 2 have distinct **L**, some have isomorphic top halves. For example, as can be seen in [4, Figure 2.2], regions F, E, I, C, and H all have isomorphic top halves. We combine these here into a single region, which we will call F. Note the different font. Similarly, regions D, B, and I′ in Fig. 2 have the same top half of **L** and are combined into a single region, D. Also, D′ and E′ combine to form D', F′ and G′ combine to F', and A, G, and H′ combine into A. This simplifies Fig. 2 into our schematic Fig. 5, which only concerns top halves of **L**. We will discuss bottom halves later in this section.

There are also curves DF, FA, DD', $D'F'$, and $F'A$ bounding these combined regions. There is also $*$, the intersection point of five curves, and the left edge $\mathcal{E}$, connecting corner points 8 and 5. In Fig. 6, we depict the top half of the cut loci for these regions, with arrows indicating convergence of points in a region to points in its boundary, in each of which an edge of the graph is collapsed.

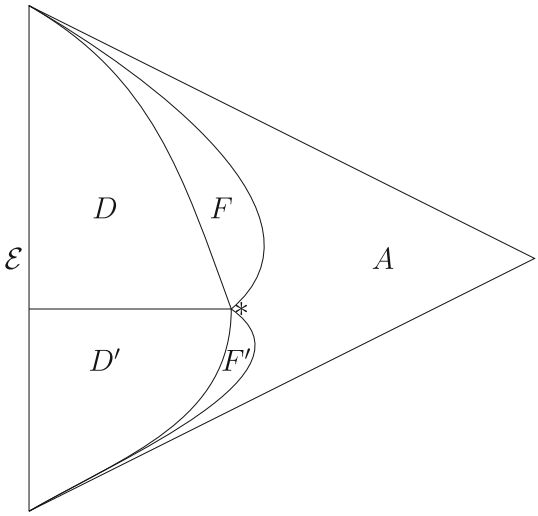

Fig. 5 Regions with same top half of **L**

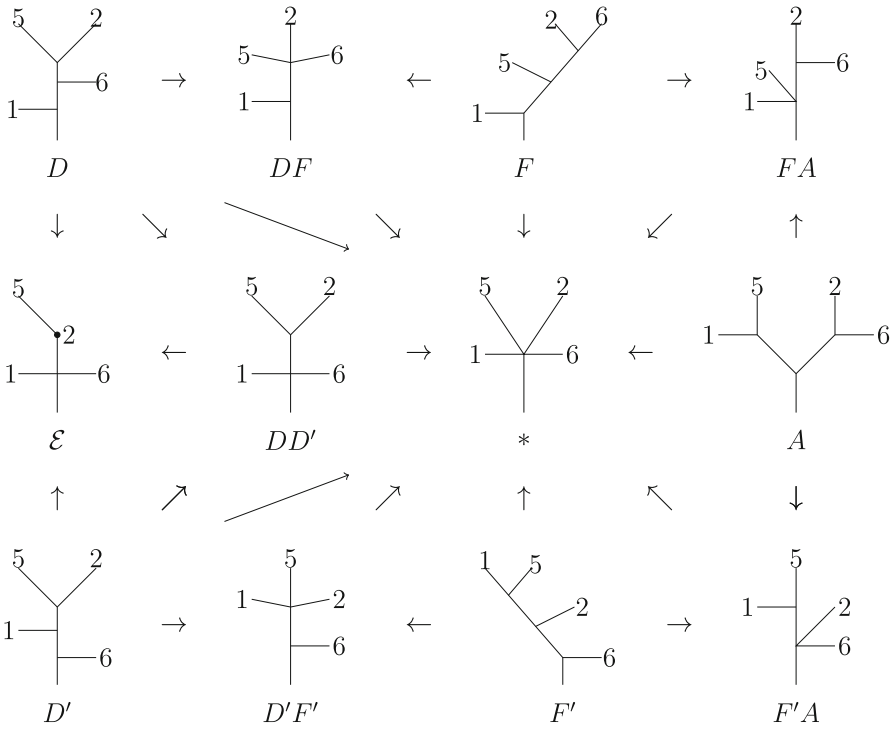

Fig. 6 Top halves of cut loci

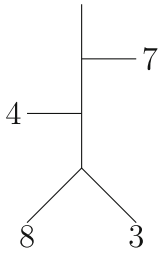

Fig. 7 Cut-locus bottom of reflection of region D' of Fig. 5

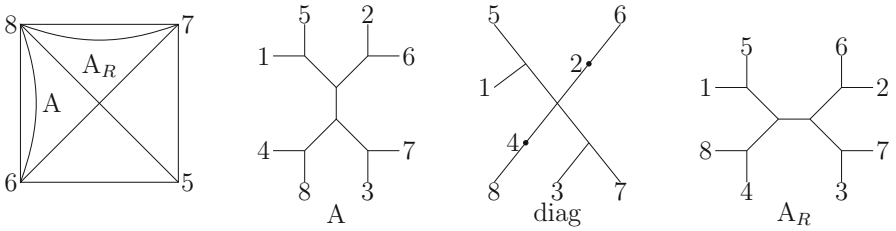

Fig. 8 Cut locus of rotation of region

The bottom half of the cut locus of a point (x, y) in a region R in Fig. 2 is obtained from the top half of the cut locus of the vertical reflection $(x, -y)$ of the point, which is in reflected region R′, by inverting it and applying the permutation (1 4)(2 3)(5 8)(6 7) to the labels. The collecting of several regions of Fig. 2 into a single region with the same bottom half of **L** is essentially a vertical reflection of what was done in forming Fig. 5 for top halves. For example, the vertical reflection of the region D' of Fig. 5 contains regions D and E of Fig. 2, and its cut locus bottom is as in Fig. 7, which is obtained by inverting the upper left diagram in Fig. 6 and applying the above permutation.

Each region in the top quadrant of Fig. 1 is obtained from the corresponding region in the left quadrant by a clockwise rotation of $\pi/2$ around the center of the square. The cut locus of the new region is obtained from that of the old one by applying the permutation (1 4 3 2)(5 8 7 6) to the labels and then rotating the resulting figure $\pi/2$ counter-clockwise. In Fig. 8, we show the cut locus of points in region A, in the rotated region A_R, and in the half-diagonal separating them.

In [4], we were only concerned about isomorphism type as a graph, but here we care about the relative positions of the labeled arms.

3 Geodesic motion-planning rules

In this section, we construct five geodesic motion-planning rules for the cube. The remainder of this section is devoted to the proof of the following result.

Theorem 3.1 *If X is the cube, then $X \times X$ can be partitioned into five locally compact subsets E_i with a GMPR ϕ_i on each.*

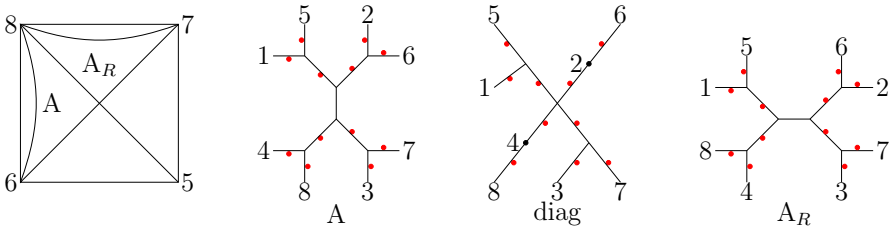

Fig. 9 Direction for ϕ_2 for some cut loci

3.1 The set E_1

We define E_1 to be the set of pairs (P, Q), such that there is a unique minimal geodesic from P to Q, and let $\phi_1(P, Q)$ be that path. It is well known ([2, Chapter 1, 3.12 Lemma]) that such a function is continuous. Note that a corner point V at a leaf of the cut-locus graph of a point P is not in the cut locus, so these (P, V) are in E_1.

3.2 The set E_2

We define the *multiplicity* of (P, Q) (or of just Q if P is implicit) to be the number of distinct minimal geodesics from P to Q. If Q is in the interior of an edge (resp. is a vertex) of the cut-locus graph of P, then the multiplicity of (P, Q) equals 2 (resp. the degree of the vertex).

We define E_2 to be the set of all (P, Q) of multiplicity 2. The points Q will be interiors of edges of the cut-locus graph or occasionally a degree-2 vertex, such as vertex 2 in the cut locus of $\mathcal{E}$ in Fig. 6. The function ϕ_2 is defined below using an orientation of the cube, i.e., a continuous choice of direction of rotation around each point.

The cut loci of points in a quadrant are a tree consisting of two parts connected by a segment parallel to the edge of the quadrant. See, for example, the cut loci of points in regions A and A_R pictured in Fig. 8. For a three-dimensional example, see Fig. 3. See Sections 5 and 6 of [5], which contains more detail than [4], for a proof. For points P on the diagonals separating quadrants, the connecting "segment" in L_P consists of a single point. See the middle diagram in Fig. 8.

Think of rotating the cut locus around the center of the connecting segment in the direction given by the orientation. If Q is not on the connecting segment, we define $\phi_2(P, Q)$ to be the geodesic from P to Q which approaches Q in the direction of the rotation. We will deal with the connecting segments shortly.

In Figs. 9 and 10, we add to Figs. 8 and 6 red dots on the edges of several cut loci indicating the side from which Q should be approached if the orientation is clockwise.

Regarding the connecting segments, note that each edge of the cube bounds two quadrants, and all L_P for P in those two quadrants have parallel connecting segments. For each quadrant pair, arbitrarily make a uniform choice of a side of these segments. Let $\phi_2(P, Q)$ for Q in those connecting segments be the minimal geodesic from P to Q which approaches Q from the selected side. Because the quadrants are bounded

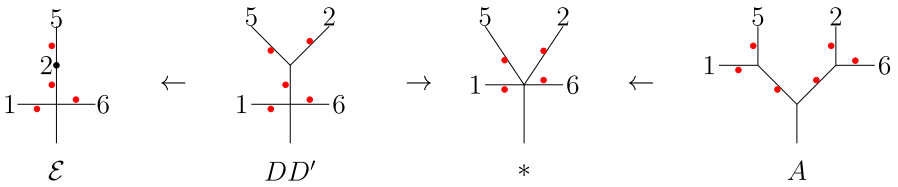

Fig. 10 Direction for ϕ_2 in some top halves

by diagonals in which the connecting points of cut loci halves are vertices of degree 4 and so are not part of E_2, compatibility of the GMPRs for connecting segments in distinct quadrant-pairs is not an issue.

We now discuss the continuity of ϕ_2. For P within a region of constant $\mathbf{L}$, the vertices v_i of its cut locus L_P vary continuously with P, as they are intersections of perpendicular bisectors of corresponding segments $P_\alpha P_\beta$, where P_α and P_β vary linearly with P (see [4, (3.3)]). The edges in the cut-locus graph are segments connecting two of these vertices v_i and v_j, and hence, if Q_t denotes a point $tv_i + (1-t)v_j$ for $0 < t < 1$, then Q_t varies continuously with P. The orientation of the cube determines the same side of the segment for all P in the region, and then, $\phi_2(P, Q_t)$ will be linear paths between continuously varying points in continuously varying Voronoi cells. For example, in Fig. 4, which corresponds to a point in region A of Fig. 2, let Q_t be the point a fraction t along the edge extending to the left from the point labeled 6, which is corner point 6 of the cube. Then, if the orientation of the cube is clockwise around the midpoint of segment I, $\phi_2(P, Q_t)$ would be the linear path from P_4 to Q_t, while if it is counter-clockwise, it would be from P_5 to Q_t. (Recall that all the P_α are different versions of the point P.) Since Q_t varies continuously with P, ϕ_2 is continuous on each subset of E_2 of the form

$$\{(P, Q) : P \text{ lies in a region of constant } \mathbf{L},\ Q \text{ on an open edge of } L_P\}.$$

For Q in the interior of a connecting edge of L_P, $\phi_2(P, Q)$, defined in the preceding paragraph, did not involve the orientation, but its continuity is clear from the ideas in this paragraph.

Suppose points P in an open region of constant $\mathbf{L}$ approach a curve bounding the region, such as points in region A in Fig. 8 approaching a point P_0 in the half-diagonal in that figure. The Voronoi diagram, such as Fig. 4, of points P will approach the Voronoi diagram of P_0. For example, the segment I in Fig. 4 collapses to a point, and the segment to the left of point 6 approaches the horizontal segment connecting 6 and 2. The paths $\phi_2(P, Q_t)$, for Q_t on this limiting segment, will still be linear paths from P_4 or P_5, depending on the selected orientation of the cube. Thus, the continuity of ϕ_2 extends from the open regions to their closures.

The cut locus of a corner point consists of the three edges and three diagonals emanating from the opposite corner point. Although continuous variation of L_P with P is not quite true when P is a corner point, we show that our defining ϕ_2 on E_2 using rotation around a central point is still continuous at the corner point. In Fig. 11, we depict the cut loci of corner point V_8 and of points P close to V_8 along the 5–8 edge,

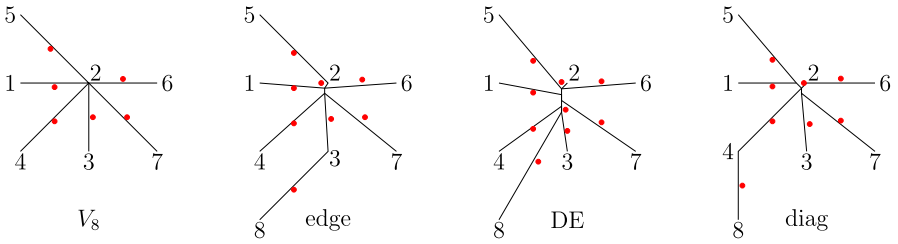

Fig. 11 Cut locus of a corner point and of points near it

along the curve DE in Fig. 2, and along the diagonal, adorned with red dots indicating the direction from which the side should be approached using ϕ_2. As we will explain, DE is supposed to be illustrative of all points between the edge and diagonal near V_8.

The points (V_8, Q) which are in E_2 are those for which Q lies in the interior of the six segments in the V_8 diagram in Fig. 11. Continuity of ϕ_2 at these points follows similarly to that at other points as discussed earlier in this subsection. Limits of points (P, Q) in E_2 with P approaching V_8 and Q on the edge of L_P emanating from vertex 8 will not have (V_8, Q) in E_2, and hence, continuity at the limit point is not an issue.

For all points P on the 5–8 edge, excluding its endpoints, points Q on the edge from vertex 8 to vertex 3 are part of L_P. However, these points Q are not in L_{V_8}, and so, (V_8, Q) is in E_1. A similar situation holds for P in the diagonal of face 5678, where L_P is pictured on the right side of Fig. 11, and the edge from vertex 8 to vertex 4 is not in L_{V_8}.

As P moves from the 5–8 edge toward the diagonal, the end point of the cut-locus edge from vertex 8 moves along the cut-locus segment emanating from vertex 3 until it meets the end point of the cut locus segment emanating from vertex 4. In the DE diagram, it is just shy of this meeting. Then, it moves along the cut-locus segment emanating from vertex 4 until it reaches vertex 4 when P is on the diagonal.

As these P approach V_8, the limit of this portion of L_P is on a segment from V_8 to a point on edge 3–4 followed by a segment down to V_2. All such limiting points (V_8, Q) are in E_1.

3.3 The set E_3

The set E_3 consists of 56 points (P, Q), such that Q is a vertex of the cut locus of P of degree 5 or 6. Since this is a discrete set, the function ϕ_3 can be defined arbitrarily. Eight of these points have P a corner point of the cube and Q the opposite corner point. The cut locus of a corner point was depicted in the left side of Fig. 11.

Another point in E_3 has P equal to the point $*$, which was introduced in Fig. 5. The top half of its cut locus is shown in Fig. 6; we show its entire cut locus in Fig. 12.

For $P = *$ and Q the indicated degree-5 vertex, we place (P, Q) in E_3. The vertical reflection $*'$ of $*$ has cut locus a reindexed vertical reflection of Fig. 12, and we place $(*', Q')$, where Q' is its degree-5 vertex, in E_3. Each quadrant has two analogous points in E_3. There are 24 quadrants, so 48 such points altogether.

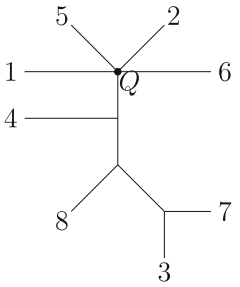

Fig. 12 Cut locus of $*$

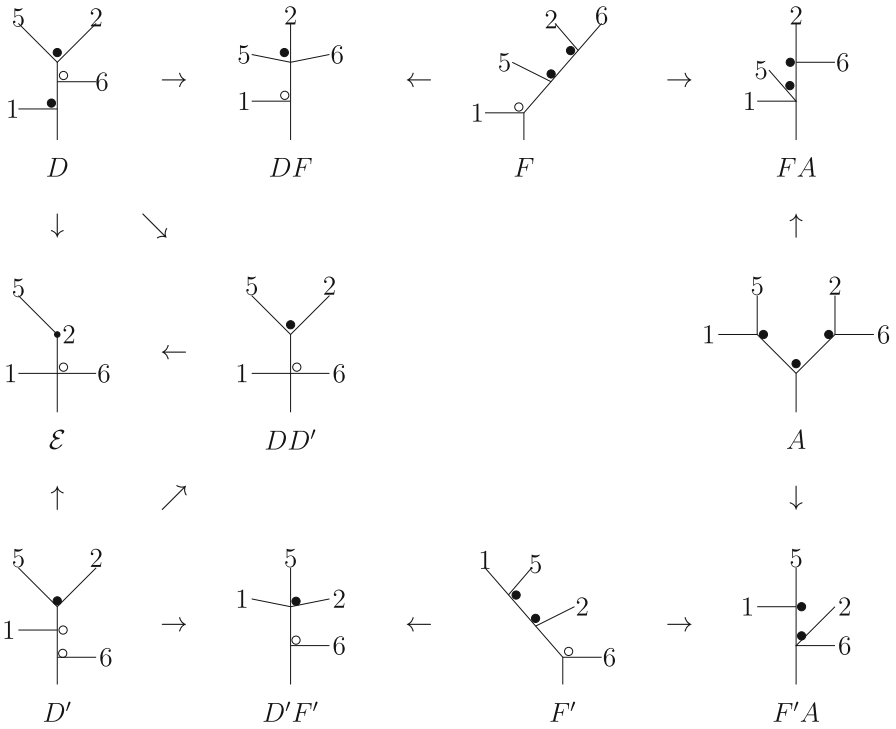

Fig. 13 Approach to vertices of cut loci

3.4 The sets E_4 and E_5

Two more sets, E_4 and E_5, are required for (P, Q) with Q a vertex of degree 3 or 4 of the cut locus of P. In Fig. 13, we depict this for Q in the top half of cut loci of points P in the left quadrant of the 5678 face. Because the degree-5 vertex in the cut locus of $*$ has been placed in E_3, we need not worry about continuity as $*$ is approached.

We place in E_4 all (P, Q) in which Q can be approached from the 2–5 region, and depict them by solid disks. For example, comparing the diagram labeled A in Fig. 13 with Fig. 4 shows how our schematic **L** correspond to actual cut loci. The

three degree-3 vertices in A in Fig. 13 correspond to three vertices in Fig. 4 which are very close together. The segments coming from vertices 1 and 5 meet at a point just to the left of the top of segment I. The paths $\phi_4(P, Q)$ for Q any of these three vertices are the segments from P_3 in Fig. 4. The "2–5 region" means the region between the segments of either of these diagrams emanating from vertices 2 and 5. The black dots in Fig. 13 indicate that for these vertices Q of the cut locus, $\phi_4(P, Q)$ is the path from P_3 in Fig. 4, the path passing between vertices 2 and 5. In Sect. 3.2, we showed that the points Q vary continuously with P, implying continuity of ϕ_4.

In E_5, we place those (P, Q) not in E_4 which can be approached from the 2–6 region, and depict them by open circles. In Diagram A in Fig. 13, the rightmost degree-3 vertex can be approached from the 2–6 region, but has already been placed in E_4. In Diagram F' in Fig. 13, the intersection points have changed and now, the end of the segment from 6 can no longer be approached from P_3 in the analogue of Fig. 4, so we choose to approach it from P_4, the 2–6 region.

The cases, in D, F, and DF, where certain Q cannot be approached from the 2–5 or 2–6 regions are placed in E_4 or E_5 as indicated by $\bullet$ or $\circ$. For example, the point (P, Q) with Q the vertex at the end of the edge from vertex 1 in Diagram D could not have been placed in E_5, because they approach a DD' diagram in E_5 whose ϕ_5 path is impossible for them to approach. Note that the degree-2 vertex when P is on the edge $\mathcal{E}$ is in E_2, which was already considered. The GMPRs ϕ_4 and ϕ_5 choose the minimal geodesic from P to Q which approach Q from region 2–5, 2–6, or 1–5.

Each arrow in Fig. 13 represents points P in a region approaching points in its boundary. A segment in a cut locus shrinks to a point. Continuity of ϕ_4 and ϕ_5 follows similarly to that of ϕ_2.

All quadrants of all faces are handled similarly, using permutations of corner-point numbers. In particular, if P is in the analogue of the large region A in any quadrant, and Q is a vertex of the top half of the cut locus of P, then (P, Q) is placed in E_4. For the degree-3 and degree-4 vertices Q of the cut locus of points P in the diagonals of a face (see Fig. 8), we place (P, Q) in E_5. Then, since A is the only region abutting the diagonal, then there is no worry about continuity of ϕ functions at these points, as long as we make consistent choices. The cut locus of the center of a face has four arms emanating from a central vertex, with a degree-2 vertex on each arm. In the 5678 face, it is obtained from the cut locus of the diagonal pictured in Fig. 8 by collapsing the arms from 1 and 3 to a point. We make an arbitrary choice of $\phi_5(P, Q)$ when Q is the degree-4 vertex of the cut locus of the center P of a face, and then choose $\phi_5(P, Q)$ compatibly when Q is the degree-4 vertex of the cut loci of points P on the diagonals of the face.

In the paragraph following Fig. 6, we described how bottom halves of cut loci are determined from top halves of cut loci. We put these (P, Q) with Q a vertex of degree 3 or 4 in the bottom half of the cut locus of P in sets E_i with GMPRs ϕ_i, $4 \leq i \leq 5$, analogously to what was done for the top halves.

The cube is composed of 12 regions such as that in Fig. 14, each bounded by half-diagonals of faces, and symmetrical about an edge of the cube. For cut-locus vertices of degree 3 or 4, the GMPRs on the diagonals are in separate sets (E_5) from those (E_4) on the A-regions abutting them, and so the 12 regions can be considered separately. Once we have defined the GMPRs for P in the region containing the 5–8

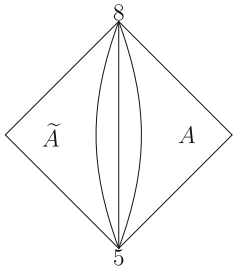

Fig. 14 A subset of the cube

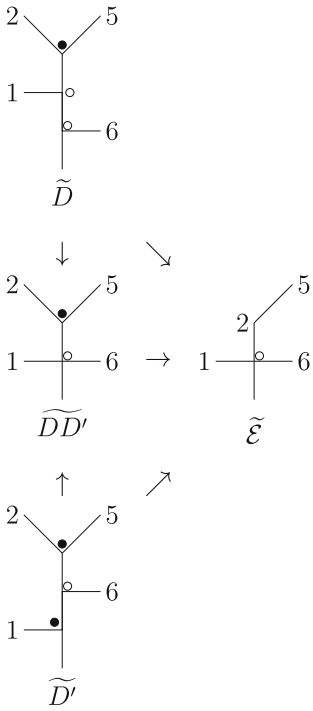

Fig. 15 Horizontal reflection

edge, GMPRs on the other regions can be defined similarly, using permutations of corner-point numbers.

The cut locus of a point $\widetilde{P}$ on the left half of Fig. 14 is obtained from that of its horizontal reflection by applying the permutation $(1\,6)(4\,7)$ and reflecting horizontally. In Fig. 15, we show top halves of cut loci for points in the reflection of the edge $\mathcal{E}$ and of the regions abutting it, together with their GMPRs for vertices of degree ≥ 3. Note that $\mathcal{E} = \widetilde{\mathcal{E}}$, so they have the same cut loci, but the depictions of them from the star unfolding are different depending on whether they are the left or right edge.

The sets E_i and functions ϕ_i, $4 \leq i \leq 5$, for the left side of Fig. 14 are defined like those on the primed (or unprimed) version on the right side, with 2 and 5 interchanged. Compare $\widetilde{D'}$ (resp. $\widetilde{D}$) in Fig. 15 with D (resp. D') in Fig. 13. This completes the proof of Theorem 3.1.

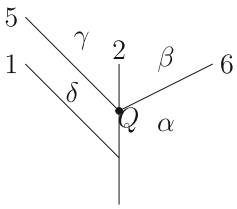

Fig. 16 Top half of cut locus of points on curve DE

4 Lower bound

In this section, we prove the following result, which is the lower bound in Theorem 1.1. The method is similar to that developed by Recio-Mitter [8] and applied by the author in [3].

Theorem 4.1 *If X is a cube, it is impossible to partition $X \times X$ into sets E_i, $1 \le i \le 4$, with a GMPR ϕ_i on E_i.*

The proof involves many subsequences and uses the following elementary lemma.

Lemma 4.2 *If a sequence x_n approaches V, and for all n, there are sequences $x_{n,m}$ approaching x_n, then, there exist increasing sequences n_k and m_k, such that $\lim_k x_{n_k,m_k} = V$, and we have $\lim_\ell x_{n_k,m_\ell} = x_{n_k}$.*

Remark 4.3 We will abuse notation and say that in the situation of this lemma, there is a diagonal subsequence with $x_{n,n} \to V$. In cases of multiple subscripts, the limit is taken over the final subscript.

We will apply this to situations where each x is a pair (P, Q).

Proof of Theorem 4.1 Assume such a decomposition exists. Note that the specific E_i of the previous section are not relevant here. Let V_i be the corner point numbered i in our treatment of the cube. The cut locus of V_8 is as in the left side of Fig. 11. It consists of edges of the cube from V_2 to V_1, V_3, and V_6, and diagonals of a face from V_2 to V_4, V_5, and V_7.

Let E_1 be the set containing (V_8, V_2), and suppose $\phi_1(V_8, V_2)$ is the geodesic passing between V_3 and V_4. Other cases can be handled in the same way, using a permutation of corner points.

Points P on the curve DE of Fig. 2 have top half of cut loci as in Fig. 16. (This is part of the curve DF in Fig. 5.)

Let Q be the vertex of degree 4 in L_P, and α, β, γ, and δ the four regions of approach to Q, as indicated in the figure. As P approaches V_8 along DE, Fig. 16 approaches the top half of the cut locus of V_8 (Fig. 11); the segment from Q to V_2 shrinks to the point V_2, and the other vertical segment collapses, too. Suppose there were a sequence of points P_n on DE approaching V_8 with Q_n the degree-4 vertex in L_{P_n}, as illustrated by the point Q in Fig. 16, and $(P_n, Q_n) \in E_1$. Then, $\phi_1(P_n, Q_n)$ would approach $\phi_1(V_8, V_2)$, but this is impossible, since they pass through different regions. Therefore, there must be a sequence P_n on DE approaching V_8 for which (P_n, Q_n) is in a different set, E_2, and restricting further, we may assume that $\phi_2(P_n, Q_n)$ all pass through the same region, α, β, γ, or δ.

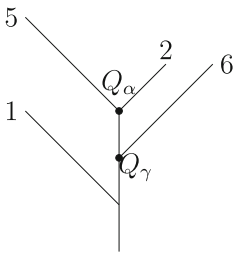

Fig. 17 Top half of cut locus of points P in region D

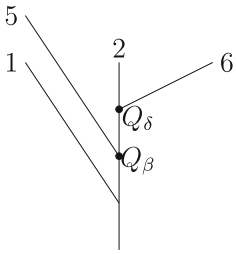

Fig. 18 Top half of cut locus of points in region E

Points in region D have top half of cut locus as in Fig. 17. See Fig. 6.

Let Q_α and Q_γ be the indicated vertices in Fig. 17; i.e., Q_α is the point in L_P where edges from V_5 and V_2 intersect, and similarly for Q_γ. If $\phi_2(P_n, Q_n)$ passes through region α (resp. γ) in Fig. 16, consider a sequence of points $P_{n,m}$ in region D approaching P_n, and let the associated cut-locus points $Q_{n,m}$ be the Q_α (resp. Q_γ) just defined. Such a sequence $(P_{n,m}, Q_{n,m})$ cannot have a convergent subsequence in E_2, since, if it did, reindexing to include just the points in the subsequence, $\phi_2(P_{n,m}, Q_{n,m}) \to \phi_2(P_n, Q_n)$, but paths going to Q_α (resp. Q_γ) cannot approach a path passing through region α (resp. γ) in Fig. 16. Therefore, we may restrict to points $(P_{n,m}, Q_{n,m})$ not in E_2, and restricting further, we may assume that they are in the same E_i for all n and m. If $i = 1$, then by Lemma 4.2 and Remark 4.3, a subsequence $(P_{n,n}, Q_{n,n})$ would approach (V_8, V_2) and would have $\phi_1(P_{n,n}, Q_{n,n}) \to \phi_1(V_8, V_2)$, which is impossible, since these paths pass through different regions. Thus, all $(P_{n,m}, Q_{n,m})$ must be in either E_3 or E_4, and we may assume that they are all in E_3.

A similar argument works if all $\phi_2(P_n, Q_n)$ pass through region β or δ in Fig. 16, using points $P_{n,m}$ in region E of Fig. 2 approaching P_n, and $Q_{n,m}$ the intersection points in $L_{P_{n,m}}$ illustrated by Q_β or Q_δ in Fig. 18, which depicts the top half of the cut locus of points in region E of Fig. 2. (Region E of Fig. 2 is part of region F of Fig. 5.) Thus, we conclude that all $(P_{n,m}, Q_{n,m})$ are in E_3, regardless of whether $\phi_2(P_n, Q_n)$ passed through α, β, γ, or δ.

Suppose all $\phi_2(P_n, Q_n)$ pass through region α in Fig. 16, and $Q_{n,m}$ are the intersection points in $L_{P_{n,m}}$ corresponding to Q_α in Fig. 17. An argument similar to the one that we will provide works if α is replaced by β, γ, or δ. All that matters is that the vertex Q_α (or its analogue) has degree 3. In Fig. 19, we isolate the relevant portion of Fig. 17, with $Q_{n,m}$ at the indicated vertex.

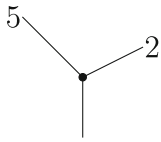

Fig. 19 A portion of Fig. 17, the cut locus of $P_{n,m}$

We may assume, after restricting, that all $\phi_3(P_{n,m}, Q_{n,m})$ pass through the same one of the three regions in Fig. 19, which we call region R. For a sequence $Q_{n,m,\ell}$ approaching $Q_{n,m}$ on the edge not bounding R, $(P_{n,m}, Q_{n,m,\ell})$ cannot have a convergent subsequence in E_3, since $\phi_i(P_{n,m}, Q_{n,m,\ell})$ cannot pass through R. Restricting more, we may assume that all $(P_{n,m}, Q_{n,m,\ell})$ are in the same E_i, with $i \neq 3$. If $i = 2$, then, using Lemma 4.2 and Remark 4.3, a subsequence $\phi_2(P_{n,m}, Q_{n,m,m})$ approaches $\phi_2(P_n, Q_n)$. Recall that as $P_{n,m}$ approaches P_n, the cut locus of $P_{n,m}$ depicted in Fig. 17 approaches that of P_n illustrated in Fig. 16. The limit of a sequence of linear paths approaching vertex Q_α $(= Q_{n,m})$ in Fig. 17 cannot pass through region α in Fig. 16, as the former lie above the cut-locus edge emanating from V_6, while the latter lie below it. Therefore, $i \neq 2$. Also, i cannot equal 1, because if so, applying Lemma 4.2 and Remark 4.3 twice, $\phi_1(P_{n,n}, Q_{n,n,n}) \to \phi_1(V_8, V_2)$, but $\phi_1(V_8, V_2)$ passes between V_3 and V_4 in the lower half of the cut locus. Therefore, $i = 4$.

We may assume, after restricting, that all the $\phi_4(P_{n,m}, Q_{n,m,\ell})$ come from the same side of the edge going out from $Q_{n,m}$ in $L_{P_{n,m}}$ which contains the points $Q_{n,m,\ell}$. Choose points $Q_{n,m,\ell,k}$ in the complement of the cut locus of $P_{n,m}$ on the opposite side of the edge converging to $Q_{n,m,\ell}$. Restricting, we may assume that all $(P_{n,m}, Q_{n,m,\ell,k})$ are in the same E_i. Note that $\phi_i(P_{n,m}, Q_{n,m,\ell,k})$ is the unique geodesic between these points. This i cannot equal 4, since $\phi_i(P_{n,m}, Q_{n,m,\ell,k})$ and $\phi_4(P_{n,m}, Q_{n,m,\ell})$ approach the edge from opposite sides. It cannot equal 3, since $\phi_i(P_{n,m}, Q_{n,m,\ell,\ell})$ and $\phi_3(P_{n,m}, Q_{n,m})$ approach the vertex in Fig. 19 from different regions. It cannot equal 2, since, applying Lemma 4.2 twice, subsequences $(P_{n,m}, Q_{n,m,m,m}) \to (P_n, Q_n)$, but $\phi_i(P_{n,m}, Q_{n,m,m,m})$ and $\phi_2(P_n, Q_n)$ approach the vertex in Fig. 16 from different regions. And, it cannot equal 1, since $\phi_i(P_{n,n}, Q_{n,n,n})$ and $\phi_1(V_8, V_2)$ approach V_2 from different regions. Therefore, a fifth E_i is required. □

Declarations

Conflict of interest We have no conflict of interest, nor do we have any financial support.

References

1. Agarwal, P., Arnov, B., O'Rourke, J., Schevon, C.: Star unfolding of a polytope with applications. SIAM J. Comput. **26**, 1689–1713 (1997)
2. Bridson, M.R., Haefliger, A.: Metric Spaces of Non-positive Curvature. Grundelehren der Mathematischen Wissenschaften, vol. 319. Springer, Berlin (1999)
3. Davis, D.M.: Geodesic complexity of a tetrahedron. Grad. J. Math. **8**, 15–22 (2023)
4. Davis, D.M., Guo, M.: Isomorphism classes of cut loci for a cube. Discrete Math. **347**, Paper No. 113709, 10 pp (2024)
5. Davis, D.M.,Guo, M.: *Isomorphism Classes of Cut Loci for a Cube*. arXiv:2301.11366v1
6. Farber, M.: Topological complexity of motion planning. Discrete Comput. Geom. **29**, 211–221 (2003)

7. O'Rourke, J., Vilcu, C.: Cut locus realizations on convex polyhedra. Comput. Geom. **114**, paper 102010, 10 pp (2023)
8. Recio-Mitter, D.: Geodesic complexity of motion planning. J. Appl. Comput. Topol. **5**, 141–178 (2021)
9. Sharir, M., Schorr, A.: On shortest paths in polyhedral spaces. SIAM J. Comput. **15**, 193–215 (1986)